13th ewtec 2019 Proceedings of the 13th European Wave and Tidal Energy Conference 1-6 Sept 2019, Naples, Italy

Power control strategies for a smoother power output from a wave power plant

Sara Anttila, Dalmo Cardoso da Silva Júnior, Irina Temiz, Janaína G. Oliveira, Jennifer Leijon, Arvind Parwal and Cecilia Boström

Abstract— **This paper presents power output and power control strategies for a wave power plant. Three cases are presented; active power output without power smoothing control, active power output with an energy storage to smooth the power output to the grid, active and reactive power control using the grid side inverter and an energy storage. The model is constructed in MATLAB Simulink and is based on the wave energy converter technology developed at Uppsala University. The model input is wave height data from the Wave Hub test site, UK. The study shows that without power control, the output power is fluctuating significantly during a 60 second time period. The difference between the average power output and the maximum power peaks can be as high as a factor of 6. A battery energy storage can significantly reduce the power fluctuations, approximately ± 10 % deviation from the average power output. Even with the high intermittency of the input power, it is possible to control the active and reactive power output to the grid. Thus, it is shown that it is possible to provide grid support functions, which are needed in the transition to a higher penetration of renewable energy sources on the grid.**

Keywords—**Active and reactive power control, grid connection of wave power, power smoothing, renewable integration.**

I. Introduction

In the transition to a fossil free energy system, the integration of Renewable Energy Sources (RESs) on the electric grid is an increasingly important need. The penetration of RESs entails new challenges to grid stability, due to its intermittent nature and often Distributed Generation (DG). DG pose several challenges regarding power quality, especially in microgrids, as discussed in a recent review [1]. A balance in active and reactive power is necessary to stabilize system frequency and voltage respectively. Additionally, reactive power is needed in several inductive loads in the grid, to establish a magnetic field.

The most common RESs connected to the grid today are wind and solar energy [2]. Using an inverter to inject reactive power to the grid has previously been discussed with regards to photo-voltaic inverters for example in [3], [4] and for wind power farms in [5], [6]. However, the majority of the wind and solar power installed on the Swedish grid today are not automated to provide voltage control [7].

Wave energy is estimated to have the global theoretical potential somewhere between 8,000 and 80,000 TWh per year [8]. The installed capacity in 2017 was approximately 8 MW [9] although many of the sites are installed for research purposes and not mainly for electricity generation.

Compared to wind and solar power, the power generated by WECs is more variable over short periods of time, due to the reciprocating motion of the waves. Variations between maximum power peaks and average power flow can be higher than a factor of 10 [10]. Additionally, WECs are, due to their location, often connected to weak points in the grid. The variation in power output combined with a weak grid can cause stability problems of grid-tied inverters as the voltage fluctuates at the inverter terminals [11]. There are several ways to address the issue of voltage instability: energy storage to balance power variations, WEC placement in wave energy farm, control strategies to minimize power variations, grid reinforcement or reactive power compensation [12].

Paper ID number 1609 track GPC.

This work was supported in part by Miljöfonden, StandUP for Energy, Swedish Research Council (VR) grant number: 2015-03126, SweGRIDS , Uppsala University, and ÅForsk.

S. Anttila is with Division of Electricity, Uppsala University, Box 534, 751 21 Uppsala, Sweden (e-mail: sara.anttila@angstrom.uu.se)

D. Cardoso da Silva Júnior is with Multi-Platform Simulations Laboratory, Electrical Engineering Graduate Program, Federal University of Juiz de Fora, Juiz de Fora, MG, Brazil (e-mail: dalmo.cardoso@engenharia.ufjf.br)

I. Temiz is with Division of Electricity, Uppsala University, Box 534, 751 21 Uppsala, Sweden (e-mail: irina.temiz@angstrom.uu.se)

J. G. Oliveira is with Department of Electrical Energy, Federal University of Juiz de Fora, Brazil as well as with Division of Electricity, Uppsala University, Box 534, 751 21 Uppsala, Sweden (e-mail: janaina.oliveira@ufjf.edu.br)

J. Leijon is with Division of Electricity, Uppsala University, Box 534, 751 21 Uppsala, Sweden (e-mail: jennifer.leijon@angstrom.uu.se)

A. Parwal is with Division of Electricity, Uppsala University, Box 534, 751 21 Uppsala, Sweden (e-mail: arvind.parwal@angstrom.uu.se)

C. Boström is with Division of Electricity, Uppsala University, Box 534, 751 21 Uppsala, Sweden (e-mail: cecilia.boström@angstrom.uu.se)

The large span between peak- and average power also has to be considered when designing the power electronics (PE). Consequently, the inverters' maximum apparent power capacity will often be larger than the WEC's power output. This, in turn, means that the capacity to provide grid support by injecting reactive power is significant for WEC connected inverters. A review on different research proposals for reactive power compensation was recently published [13], highlighting the importance of the location and dimensioning of the reactive power compensation systems. Using the inverters which are already connected to the grid is a less expensive option for reactive power regulation.

Reactive power compensation for wave power systems, with its voltage fluctuations, has previously been studied [14]. Control and grid-connection of an offshore wave power farm consisting of Uppsala WECs are discussed in [15].

In this paper, three cases are presented. In Case 1 the active power output from a wave park with WEC technology devices developed by Uppsala University [16] at unity power factor is presented. In Case 2 a battery energy storage system is connected to smoothen the power output to the grid. In Case 3 the inverter is used to control the active and reactive power output on the grid.

II. Wave Power Park Modelling

The wave power park contains ten WECs which are heaving point absorbers anchored to the sea floor. The buoy is on the water surface and is connected to a power take-off system consisting of a permanent magnet linear generator, see Fig. 1. The WECs dimensions are presented in Table I.

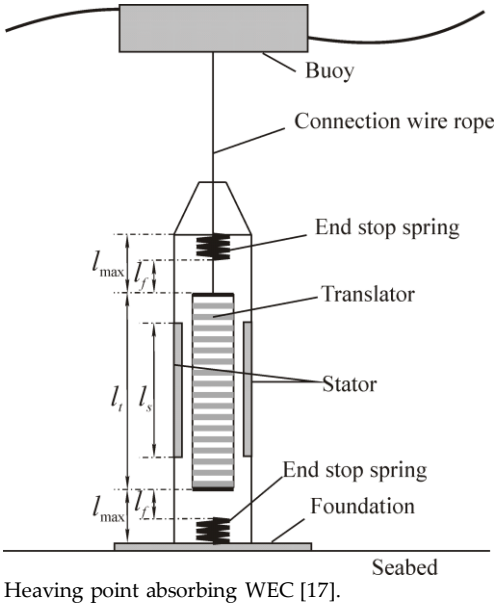

Fig. 1. Heaving point absorbing WEC [17].

TABLE I
WEC DIMENSIONS.

Parameters	Value
Mass of translator m_t (kg)	9000
Length of translator l_t (m)	3
Length of stator l_s (m)	2.164
End stop spring coefficients k_s (kN/m)	270
Wire rope spring coefficient k_w (kN/m)	833
Free stroke length l_f (m)	0.75
Maximum stroke length l_{max} (m)	1.2
Mass of buoy m_b (kg)	4400
Buoy radius r_o (m)	3
Moonpool radius r_i (m)	2.3

The WECs are connected in parallel, after rectification. The three-phase output currents from each WEC are rectified and fed into a mutual infinite DC-bus modeled as an ideal constant voltage source of 800 V with a negligibly small impedance. Fig. 2 illustrates the model of the wave power park.

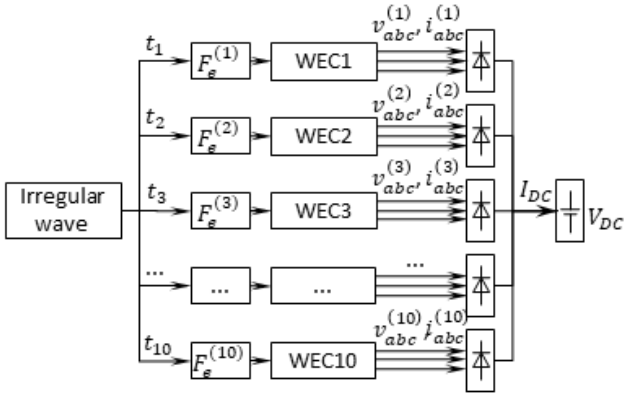

Fig. 2. Schematic of the model from wave to DC-link.

A. *Single WEC m*odel

Each WEC is modelled using Matlab/Simulink. The WEC dynamics is described by two equations coupling hydrodynamic, mechanical and electromagnetic properties of the wave power plant:

$$m_b \ddot{z}_b = F_e - F_r - F_h - F_{gb} + F_b - F_w \quad (1)$$

$$m_t \ddot{z}_t = F_w - F_d - F_{gt} + F_{es} \quad (2)$$

where m_b and m_t are the buoy and translator mass respectively, z_b and z_t denote the buoy and translator displacements, F_e is the excitation force, F_r is the radiation force, F_h is the hydrostatic stiffness force, F_{gb} and F_{gt} are the gravity forces of the buoy and the translator respectively, F_b is the buoyancy force, F_w is the wire force used for coupling between the buoy and the translator motion, F_d is the electromagnetic damping force, and F_{es} is the end stop spring force, see Fig. 3. For a detailed definition of all forces (apart from the damping force) and

input parameters, the reader is referred to [17]. The definition of the damping force F_d is given in (5).

The induced three-phase voltages in the WEC stator windings are given by

$$e_{abc} = -\frac{N\pi\hat{\phi}_{PM}}{\tau_p} \cdot \dot{z}_t \cdot \cos\left(\frac{\pi z_t}{\tau_p} + \varphi\right) \tag{3}$$

where N is the total number of turns in the stator coil, $\hat{\phi}_{PM}$ is the maximum magnetic flux from the permanent magnet, τ_p is the pole width, and φ is the phase shift between phases equal to 0, $\pm\frac{2\pi}{3}$. Then the line currents i_{abc} and the output terminal voltaes v_{abc} are calculated from

$$v_{abc} = e_{abc} - R_s i_{abc} - L_s \frac{di_{abc}}{dt} \tag{4}$$

where R_s and L_s are the stator winding synchronous resistance and reactance. The currents i_{abc} are transformed to the *dq0*-reference frame, and the quadrature current i_q is used to define the damping force on the generator

$$F_d = \frac{3\pi}{2\tau_p} N\hat{\phi}_{PM} i_q \tag{5}$$

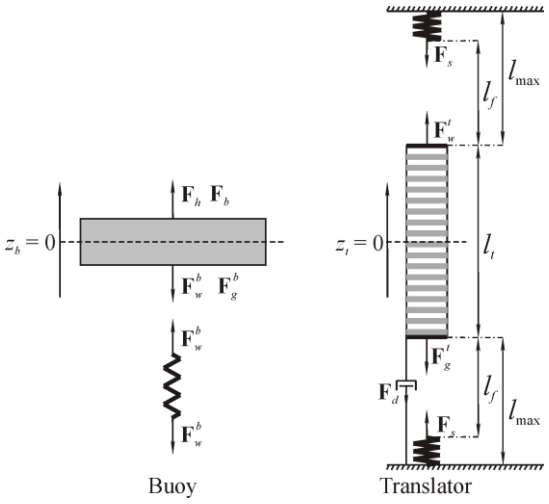

Fig. 3 Illustration of forces acting on the buoy and translator [17].

B. Input to the wave power park model

Waves were measured at Wave Hub test site, situated 16 km off the coast of Cornwall in South West England, and are available through the Channel Coastal Observatory[1]. Wave time series measured at 2017-01-28, between 03:00 and 03:30 is used as an input to the model. The significant wave height for the input data at that time is approximately 2 m, which is less than the maximum transistor displacement of 2.4 m. The peak wave period is approximately 12 s and the resonant period of the WEC is about 2.42 s [17].

From the wave time series, the corresponding excitation force is found

$$F_e = f_e(t) * \eta(t) \tag{6}$$

where f_e is the excitation force transfer function, and η is the incident wave at the location of the WEC.

Since the focus of the current paper is on the output power management strategy, none hydrodynamic interaction between WECs is employed here. Instead, we assume that the same incident wave reaches WECs at different (randomly generated) time instants with the greatest time difference of 20 s. From the 30 minute period, over which the wave power park model is simulated, a 60 second period of high intermittency is chosen for control analysis.

III. Inverter Modelling

The inverter was modelled as three-phase and two-levels with IGBT switches, see Fig. 4. A sine-pulse width modulator (SPWM) with a switching frequency of 24 kHz generates the switching signals to the inverter. The grid is assumed to be balanced and modelled as an ideal three-phase source.

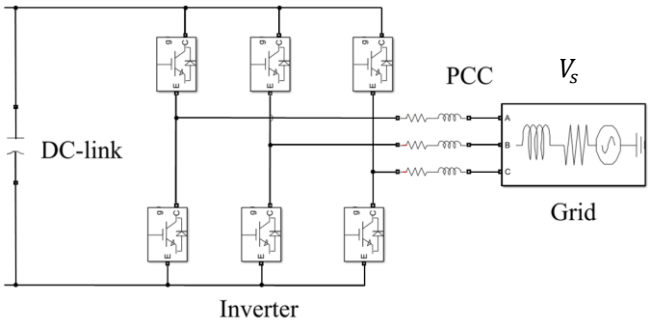

Fig. 4. Three-phase two-level grid connected inverter.

C. PI controllers

The transfer functions ($E(s)/E_i(s)$) in the Laplace domain for the PI controllers are given by

$$\frac{E(s)}{E_i(s)} = K_p + \frac{K_i}{s} \tag{7}$$

where K_p is the proportional gain and K_i is the integral gain as described in [18]. The values for K_p and K_i for the PI controllers used are presented in Table II.

[1] http://www.channelcoast.org/, Accessed 2019-02-18.

TABLE II
K_p AND K_i VALUES FOR PI CONTROLLERS

Parameters	Quantity
K_p Case 1	0.3127
K_i Case 1	187.7
K_p voltage error, Cases 2 & 3	100
K_i voltage error, Cases 2 & 3	1000
K_p current error, Cases 2 & 3	0.04
K_i current error, Cases 2 & 3	2

D. DC-link voltage control

In Case 1 the DC-link voltage is controlled with a feed-forward loop, as illustrated in Fig. 6.

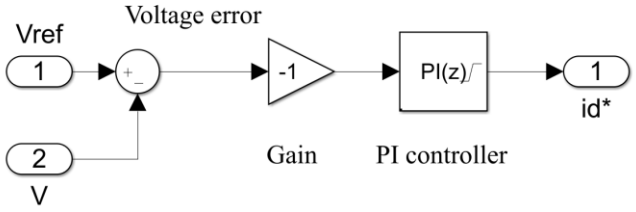

Fig. 5. Feed-forward loop for DC-link voltage control in Case 1.

In Cases 2 & 3 the DC-link voltage is controlled with a feed-forward loop, as illustrated in Fig. 5. S1 and S2 illustrates the switches to the energy storage. V_{dc} is the DC-link voltage and I_{dc} is the battery current. A detailed description of the control method can be found in [19]. The DC-link reference voltage is set to 800 V. The DC-level voltage has an impact on the energy absorption of the WECs [20]. The voltage level of 800 V DC is chosen due to the grid voltage (220 V_{RMS}). To maximize the power absorption, a lower DC voltage in combination with a DC/DC boost converter would have to be used.

E. Active and reactive power control

The active and reactive power are controlled with a current-mode, grid-imposed frequency voltage source converter (VSC). The control strategy is thoroughly described in [19]. The VSC line current is regulated by a feedback of the AC-side terminal voltage. The active and reactive power output (P_s and Q_s) are controlled with the VCS line current as [19]:

$$P_s(t) = \frac{3}{2}[V_{sd}(t)i_d(t) + V_{sq}(t)i_q(t)] \tag{8}$$

$$Q_s(t) = -\frac{3}{2}[V_{sd}(t)i_q(t) + V_{sq}(t)i_q(t)] \tag{9}$$

where V_{sd} and V_{sq} are the dq-frame grid-side voltage components, i_d and i_q are dq-frame grid-side current components.

When the phase-locked-loop (PLL) is in steady state, $V_{sq} = 0$. Thus, as can be seen from (8) and (9), i_d and i_q can be used to control P_s and Q_s as:

$$i_{dref}(t) = \frac{2}{3V_{sd}}P_s(t) \tag{10}$$

$$i_{qref}(t) = -\frac{2}{3V_{sd}}Q_s(t) \tag{11}$$

Using the disposable apparent power output from the inverter (S_{inv}), Q_{inv} for each P_{WEC} can be calculated as:

$$Q_{inv}^2 \leq \sqrt{S_{inv}^2 - P_{WEC}^2} \tag{12}$$

Verification of the active and reactive power control is done by calculating the phase shift (ϕ) between the voltage and current according to:

$$\phi = 2\pi\Delta t f \tag{13}$$

where Δt is the lag time between the voltage and current and f is the system frequency.

F. Energy storage

A battery energy storage is chosen in this study. The dimensions are presented in Table III. The focus has not been to optimize the dimensioning of the energy storage in this study.

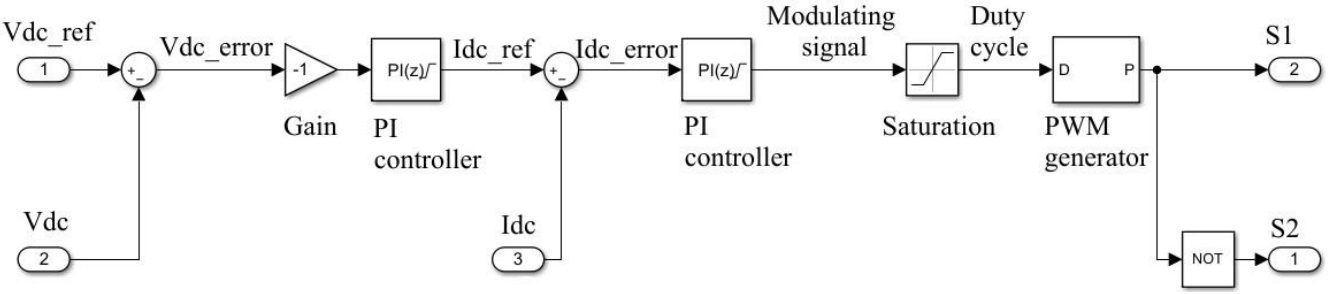

Fig. 6. Feed-forward loop for DC-link voltage control in Case 2 & 3.

TABLE III
BATTERY STORAGE

Parameters	Quantity	Unit
Type	NiCd	
Nominal Voltage	500	V
Nominal discharge current	1.1	A
Rated capacity	5.4	Ah
Initial State-of-Charge	50	%
Battery Response Time	30	s

IV. RESULTS

The power output from the wave power park after the passive rectification during 30 minutes is presented in Fig. 7. The average power output is approximately 5 kW, whereas the maximum peak power is around 130 kW.

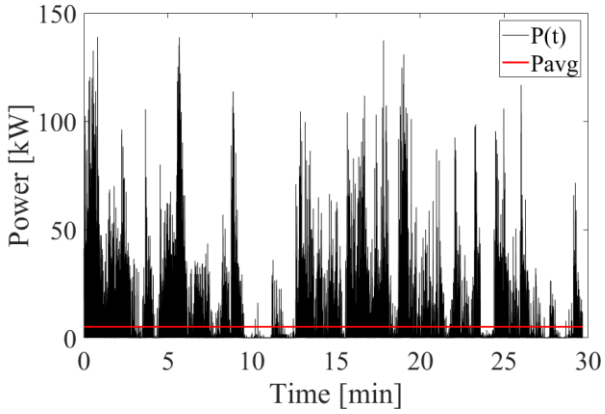

Fig. 7. Power output from wave power park.

The first 60 seconds contain high intermittency and are chosen to analyse the control. The power output from the wave power park after the passive rectification is presented in Fig. 8. During this time the average power is 20 kW and the maximum power is still approximately 130 kW.

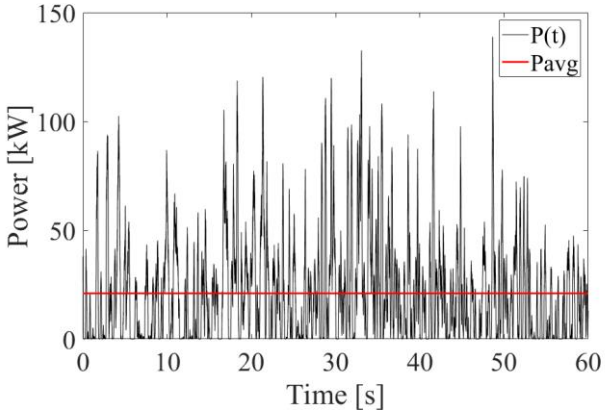

Fig. 8. Power output from the wave power park.

1) *Case 1 - Active power output without energy storage at unity power factor*

The study shows that the power output is highly fluctuating, where the difference between the average power output and the maximum power peaks can be as high as a factor of 6, the power profile is shown in Fig. 9.

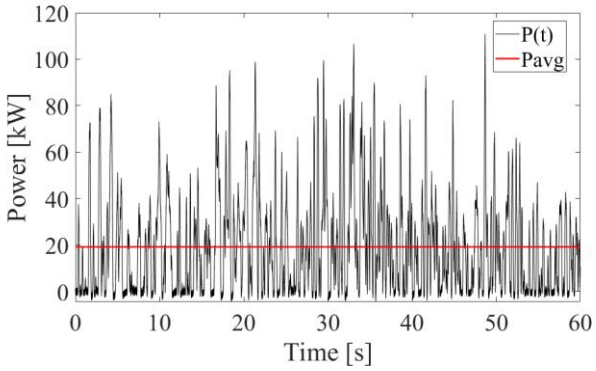

Fig. 9. Power output to the grid, without energy storage for power smoothing (Case 1).

The control is working as desired, the DC-link voltage is maintained close to the reference voltage of 800 V, as shown in Fig. 10.

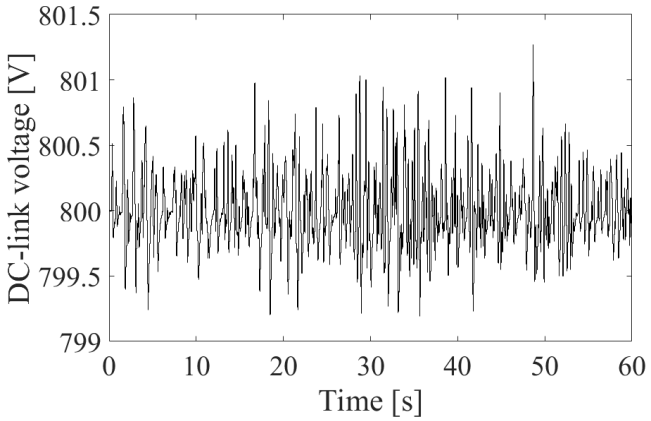

Fig. 10. DC-link voltage in Case 1, where the reference voltage is 800 V.

2) *Case 2 – Power smoothing using an energy storage*

A constant $i_{d\_ref} = 43\ A$ is chosen to correspond to the average power output in Case 1 (20 kW). Reactive power is set to 0 ($i_{q\_ref} = 0\ A$). As shown in Fig. 11 & Fig. 12the average power output is about 20 kW where the power fluctuates between approximately 18.5 and 21.5 kW. As can be seen, the power fluctuations are greatly reduced from a factor of 6 in Case 1 (Fig. 9) to approximately ± 10 % with the implemented control and battery energy storage. The DC-link voltage is still maintained at a desired level as can be seen in Fig. 13.

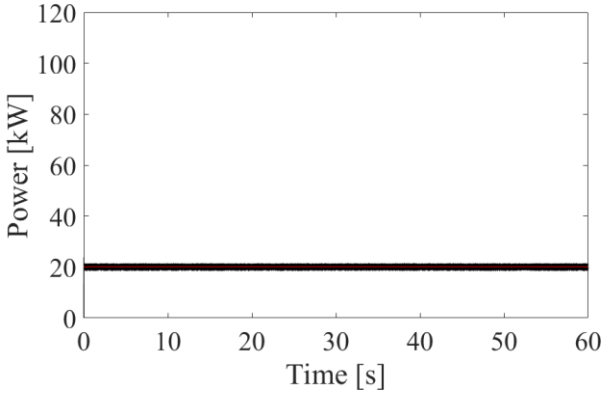

Fig. 11. Active power output from the wave power park to the grid with energy storage (Case 2).

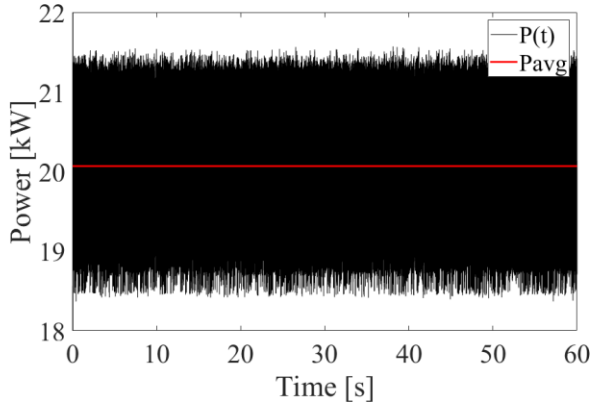

Fig. 12. Detailed view of active power output from the wave power park to the grid with energy storage (Case 2).

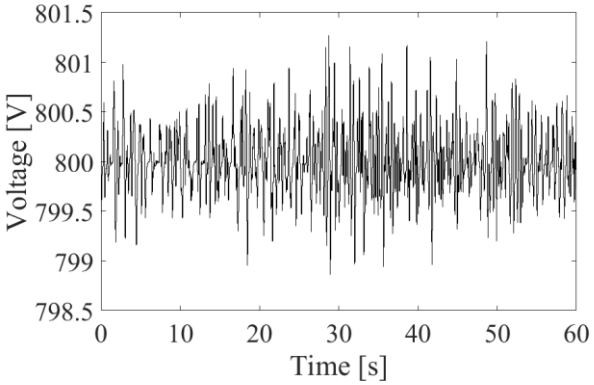

Fig. 13. DC-link voltage in Case 2, where the reference voltage is 800 V.

3) *Case 3 – Active and reactive power control*

The active and reactive power is controlled as shown in (10) & (11) respectively. The same apparent power as in Case 2 is chosen (20 kVA) and the power factor (PF) is set to 0.85. Thus, the reference currents are set to $i_{d\_ref} = 36.6\,A$ and $i_{q\_ref} = 22.7\,A$ according to (10), (11) & (12). The voltage (V_a) and current (I_a) in one phase is shown in Fig. 14.

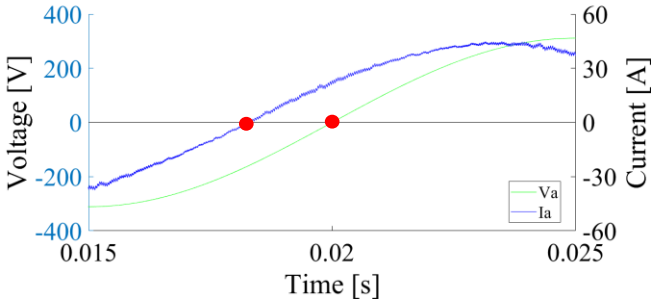

Fig. 14. Phase shift for voltage and current for PF=0.85.

Using (13) where $\Delta t = 0.0018$ s and $f = 50$ Hz, $PF = 0.84$ which is an insignificant deviation from the input $PF = 0.85$.

V. Discussion

The results for Case 1 show that the power output from the wave power park is highly intermittent. Connecting an energy storage, as in Case 2, is one way to smoothen the power output to the grid. Another possibility, which has not been implemented in this study is to use active rectification to smoothen the DC current in the DC-link. Modifying the wave power park layout is another factor which could affect the power output from the wave power park. This has not been accounted for in this study (randomized excitation forces have been used), but merits attention in further development of the model.

The voltage level of 800 V was chosen with regards to the grid. To optimize the power output from the wave power park a lower DC-link voltage would be needed, combined with a DC/DC boost converter before the grid side inverter.

The control of active and reactive power, as is done in Case 3, show that although the source may be highly intermittent, it is possible to control active and reactive power output to the grid. However, this is solely a proof of concept. To be able to provide grid support by reactive power compensation it is necessary to get input from the grid, which is not done in this study.

The control strategies presented here assumes a stable grid i.e. that the system inertia regulates the frequency and that the production and load is balanced. A higher penetration of intermittent distributed RES with low inertia will challenge the grid stability. Thus further development of the control strategy will be needed.

VI. Conclusion

This paper presents a wave-to-wire model of a wave power park consisting of 10 WECs. The WECs are heaving point absorbers anchored to the sea floor, based on devices developed in Uppsala University. The power output from the wave power plant is shown to be highly intermittent when regulation is not implemented. To smoothen the power output a battery energy storage is connected. The battery energy storage is used to keep the power output steady at the average power. The suggested control can significantly reduce the power

fluctuations, to provide a more stable output to the grid. Furthermore, an active and reactive control strategy is implemented. The results show that although the source may be highly intermittent, it is possible to control active and reactive power output to the grid. However, to fully implement reactive power compensation to the grid would require that the control system react to changes within the grid, which is not implemented in this study. The study shows that several grid support strategies from the wave power park are achievable with the use of an energy storage.

ACKNOWLEDGEMENT

D. Cardoso da Silva Júnior would like to thank the Federal University of Juiz de Fora and Electrical Engineering Graduate Program.

REFERENCES

[1] M. T. L. Gayatri, A. M. Parimi, and A. V. Pavan Kumar, "A review of reactive power compensation techniques in microgrids," *Renew. Sustain. Energy Rev.*, vol. 81, no. August 2017, pp. 1030–1036, 2018.

[2] International Renewable Energy Agency, *Renewable Energy Statistics 2018*. 2018.

[3] Y. Yang, F. Blaabjerg, H. Wang, and M. G. Simões, "Power control flexibilities for grid-connected multi-functional photovoltaic inverters," *IET Renew. Power Gener.*, vol. 10, no. 4, pp. 504–513, 2016.

[4] S. Weckx and J. Driesen, "Optimal Local Reactive Power Control by PV Inverters," *IEEE Trans. Sustain. Energy*, vol. 7, no. 4, pp. 1624–1633, 2016.

[5] M. A. Saqib and A. Z. Saleem, "Power-quality issues and the need for reactive-power compensation in the grid integration of wind power," *Renew. Sustain. Energy Rev.*, vol. 43, pp. 51–64, 2015.

[6] E. Martínez, F. Sanz, J. Blanco, F. Daroca, and E. Jiménez, "Economic analysis of reactive power compensation in a wind farm: Influence of Spanish energy policy," *Renew. Energy*, vol. 33, no. 8, pp. 1880–1891, 2008.

[7] Svenska kraftnät, "Anpassning av elsystemet med en stor mängd förnybar elproduktion - En delredovisning från Svenska kraftnät," 2015.

[8] IEA-OES executive committee, "International Energy Agency Implementing Agreement on Ocean Energy Systems: annual report 2007," 2007.

[9] IEA-OES executive committee, "Annual report, An overview of Ocean Energy activities in 2017," *Exec. Comm. Ocean Energy Syst.*, p. 154, 2017.

[10] M. Penalba and J. V. Ringwood, "A review of wave-to-wire models for wave energy converters," *Energies*, vol. 9, no. 7, 2016.

[11] A. Adib, B. Mirafzal, X. Wang, and R. Blaabjerg, "On stability of voltage source inverters in weak grids," *IEEE Access*, vol. 6, pp. 4427–4439, 2017.

[12] F. Sharkey, J. MacEnri, E. Bannon, M. Conlon, and K. Gaughan, "Resource-induced voltage flicker for wave energy converters – assessment tools," *IET Renew. Power Gener.*, vol. 7, no. 6, pp. 623–630, 2013.

[13] A. Águila Téllez, G. López, I. Isaac, and J. W. González, "Optimal reactive power compensation in electrical distribution systems with distributed resources. Review," *Heliyon*, vol. 4, no. 8, 2018.

[14] A. Medina, H. Mendonça, and S. Martinez, "Study of Voltage Fluctuations Caused in a Distribution Grid by the Connection of a Wave Energy Converter and Corrective Actions Based on Reactive Power Compensation," *Procedia Comput. Sci.*, vol. 83, no. Seit, pp. 832–838, 2016.

[15] R. Ekström and M. Leijon, "Control of offshore marine substation for grid-connection of a wave power farm," *Int. J. Mar. Energy*, vol. 5, pp. 24–37, 2014.

[16] M. Leijon *et al.*, "An electrical approach to wave energy conversion," *Renew. Energy*, vol. 31, no. 9, pp. 1309–1319, 2006.

[17] I. Temiz, J. Leijon, B. Ekergård, and C. Boström, "Economic Aspects of Latching Control for a Wave Energy Converter with a Direct Drive Linear Generator Power Take-Off," *Renew. Energy*, vol. 128, pp. 57 – 67, 2018.

[18] K. Ogata, *Modern Control Engineering*. 2001.

[19] A. Yazdani and R. Iravani, *Voltage-Sourced Converters in Power Systems - Modeling, Control, and Applications*. 2010.

[20] C. Boström and M. Leijon, "Operation analysis of a wave energy converter under different load conditions," *IET Renew. Power Gener.*, vol. 5, no. 3, p. 245, 2011.